Depth characterization of the BOLD hemodynamic response function in human early visual cortex

Reswanul Khan[1], Sucharit Katyal[2], Clint Greene[2], Evan Luther[3], and David Ress[2]

[1]Neurobiology, Physics, Imaging Research Center, Center for Perceptual Systems, The University of Texas at Austin, Austin, TX, United States, [2]Neurobiology, Psychology, Imaging Research Center, Center for Perceptual Systems, The University of Texas at Austin, Austin, TX, United States, [3]Neurobiology, Biomedical Engineering, Imaging Research Center, Center for Perceptual Systems, The University of Texas at Austin, Austin, TX, United States

Introduction. fMRI is often performed at resolutions so coarse that a voxel includes contributions from white matter, gray matter, and superficial extra-pial tissues. To better understand these measurements, we performed high-resolution fMRI (voxels < 1 mm) measurements to resolve the BOLD response within the depth of cortical tissue. These measurements identify trends that elucidate the relationship between hemodynamics and cortical structure. This will yield a more accurate interpretation of existing low-resolution brain data, and improve our understanding of the physiological mechanisms that mediate the BOLD response in the human brain.

Methods. We studied the BOLD response evoked by a brief period of brain stimulation, the BOLD hemodynamic impulse response function (HRF) (*1-5*). Stimulus was a 1.7-s duration presentation of 4-Hz flickering dots followed by a 25.3-s no-stimulus period to let the HRF evolve and subside. Each of these HRF trials was repeated 18 times in the course of ~8.5-min runs. Scanning sessions typically included 5 such runs. Subjects were required to perform a fixation-point detection task continually throughout each scanning run to control attention.

High-resolution (0.9-mm sampling) fMRI data was obtained during these sessions using a 3T GE Signa Excite scanner. Acquisition utilized a two-interleave spiral trajectory (*6-8*), on eight 0.9-mm-thick slices prescribed over a 90-mm field-of-view oriented tangentially to caudal occipital cortex so that portions of visual areas V1, V2, and V3 were included. Signal-to-noise ratio was enhanced by use of a custom (ScanMed, Omaha NE) 7-channel surface-coil array constructed in flexible former to permit a close fit to the back of each subject's head, and by reducing the bandwidth of the acquisition to 62.5 kHz so that the readout time was 27.4 ms for each interleave. Echo time was 25 ms.

We also obtained 0.7-mm isovoxel volume anatomies for five subjects using the product 8-channel head-coil and acquired with a T1-weighted 3D fast-SPGR sequence. A combination of manual methods and the FreeSurfer software suite was used to segment the white matter. We then applied a surface-based analysis method to form a normalized depth map of the brain tissue using smooth surfaces generated at the gray-white and pial interfaces. A vector field of signed-distance function from each surface was interpolated into the domain between the white and pial surfaces using a deformable-surface algorithm. This vector field provides a self-reciprocal trajectory map linking the two surfaces together; gray-matter thickness is measured upon these trajectories. Distances into the white and extra-pial tissue were calculated using a nearest-neighbor measurement with respect to the gray-white and pial surfaces, respectively. All distances were then normalized with respect to local gray-matter thickness.

The high-resolution fMRI data underwent motion, timing, and baseline corrections, and were then interpolated onto the segmented reference volume. Each session produced 72—85 HRF measurements. We chose the top 50% of activated voxels within the early visual areas. HRFs variations with depth were then obtained by rebinning (0.9-mm bin width) the time series data based on the normalized depth coordinates (Fig. 1). We extracted parameters from the HRFs obtained from each depth bin: initial-dip time and amplitude; hyperoxic peak time and amplitude; undershoot time and amplitude. Bootstrapping upon the multiple HRF measurements was used to establish confidence intervals for the time series and parameters.

Results. Time-to-peak and peak amplitude increased significantly with distance above the gray-white interface (Fig. 3). There was no significant initial dip observed in the gray matter, but the initial dip was significant in the extra-pial tissue. Undershoot amplitude also increased significantly with distance above the white matter. Undershoot times showed a complex, multi-modal distribution. In general, white matter exhibited weak HRFs, extra-pial tissue exhibited strong and noisy HRFs, while gray matter exhibited moderate-to-strong HRFs with comparatively low noise.

Conclusions. We are able to resolve strong and consistent depth variations in HRF parameters as a function of normalized depth within multiple subjects and visual areas. The BOLD HRF begins in the deepest gray matter, and then propagates more superficially, where it is stronger and less reliable.

[1]R. S. Menon, S. G. Kim, *Trends in Cognitive Sciences* **3**, 207 (1999); [2]R. Ä. Buckner *et al.*, *Proceedings of the National Academy of Sciences* **93**, 14878 (1996); [3]K. K. Kwong *et al.*, *Proceedings of the National Academy of Sciences* **89**, 5675 (1992); [4]P. A. Bandettini, E. C. Wong, R. S. Hinks, R. S. Tikofsky, J. S. Hyde, *Magn Reson Med* **25**, 390 (1992); [5]S. Ogawa *et al.*, *Proceedings of the National Academy of Sciences* **89**, 5951 (1992); [6]G. H. Glover, *Magn Reson Med* **42**, 412 (Aug, 1999); [7]G. H. Glover, S. Lai, *Magn Reson Med* **39**, 361 (Mar, 1998); [8]D. Ress, G. H. Glover, J. Liu, B. Wandell, *NeuroImage* **34**, 74 (Jan 1, 2007).

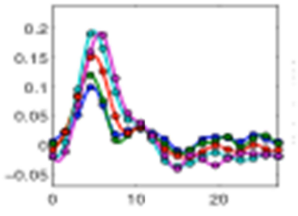

Figure 1: Laminar profiles

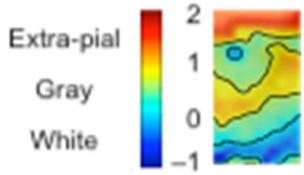

Figure 2: Normalized depth coordinates

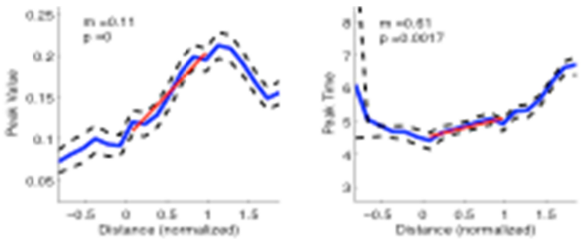

Figure 3: Parameter variations